*Minefill 2020-2021 – Hassani et al (eds)*
*© 2021 Taylor & Francis Group, London, ISBN 978-1-032-07203-6*

# Cemented paste backfill failure envelope at low confining stress

Murray Grabinsky & Andrew Pan
*University of Toronto, Toronto, Canada*

SUMMARY: A popular method to determine backfill strength for sidewall exposure assumes that the cohesive bond strength is equal to one-half the Unconfined Compressive Strength ($c_b$ = ½ UCS). A new laboratory study uses direct shear, UCS, and novel tensile strength test results to show that this strength assumption is not valid for the tested CPB (and quite possibly many other CPBs). The implications of this finding in the context of strength for exposed backfill sidewalls is investigated using generalized design examples.

*Keywords*: Exposed backfill sidewalls, strength envelope, backfill design

## 1 INTRODUCTION

Stope sequencing of an underground ore body often results in previously placed backfills having their sidewalls exposed when an adjacent unmined stope is subsequently extracted. Mitchell et al. (1982) described some historical approaches to assessing the backfill strength required for sidewall exposure and developed a new solution. The solution's validity was verified through laboratory scale tests in which model backfills had their sidewalls exposed and the nature of the failure (if any) was assessed. The material strength at the time of model testing was also determined by direct shear testing on control samples. The simplest expression of the design formula, and the one recommended for use in practice, takes the form.

$$UCS = \frac{\gamma H}{1 + \frac{H}{L}} = \frac{\gamma L}{1 + \frac{L}{H}} \tag{1}$$

where UCS is the unconfined compressive strength, γ is the backfill unit weight, and H and L are the height and strike length (respectively) of the exposed backfill face. The first term in Equation 1 is the one presented in Mitchell et al. (1982) whereas the second term (which is equivalent) will be a more convenient form later in this work. The second form also obviates the singularity that exists for H ≫ L. This design formula is elegant in its simplicity and has been widely adopted. It is less clear how mining operations apply Factors of Safety (if any) to this limiting strength formula, and how they might implement QA/QC procedures to ascertain if the design strengths are being reliably achieved in their underground operations. Regardless, the formula's widespread and successful use can be taken as a *de facto* validation of its design suitability.

Despite Equation 1's popularity, the theoretical background to its development seems to be relatively poorly understood. A particularly unusual assumption is that the strength mobilized on the backfill's sidewalls, the so-called "bond strength" $c_b$, is equivalent to one-half the UCS: i.e., $c_b$ = ½ UCS. This assumption appears to have gone unchallenged in the almost four

DOI: 10.1201/9781003205906-11

decades since publication, but for backfill it is not the typically expected form of failure criterion for a generally accepted frictional material. Therefore, the purpose of this paper is to present results of careful laboratory tests at low confining stress that show the tested material does not have a failure envelope conforming to the $c_b$ = ½ UCS assumption, and to explore the design implications of this finding. However, first a brief review of the background to Equation 1 is given to provide context to the laboratory test work.

## 2 BACKGROUND TO MITCHELL'S METHOD (EQUATION 1)

Mitchell et al. (1982) explain that prior to their studies it was commonly assumed that an exposed backfill height should be capable of supporting its own self weight (i.e., UCS = $\gamma$H), or else it would be assumed that the backfill would fail according to the model of a vertical face in clay (in which case UCS = ½ $\gamma$H). The discrepancy between these approaches was deemed unsatisfactory and hence the motivation for their original work. They recognized that neither of these previous methods accounted for the stabilizing effect of bond strength developed between the backfill and the end walls (each with width w and height H, the distance w being perpendicular to the exposed face). They decided to incorporate this stabilizing effect through a form of "arching" analysis (Terzaghi, 1967).

The term "arching" is controversial, and it is generally recognized that the internal stress distribution in such "arching" phenomenon does not correspond to the mechanical behaviour of a structural arch (Handy, 1985). For the purposes of backfill analysis it is perhaps better to describe the phenomenon as "net weight" analysis. That is, the total weight of the backfill ($\gamma$HwL) will be reduced by the sidewall stresses and result in a net weight which, when averaged over the horizontal area (wL) will give a vertical stress. If it is further assumed that the average horizontal stress at the backfill's base is zero (because the sidewall has been exposed) then this net vertical stress must be less than the material UCS. In the case of the Mitchell analysis, using the assumption $c_b$ = ½ UCS with $c_b$ acting over the two end walls with area wH, means the net vertical stress at the base is ($\gamma$HwL - $2c_b$wH)/wL and if this net vertical stress is equal to the UCS then one obtains UCS = $\gamma$H - $2c_b$H/L = $\gamma$H - UCS H/L and this is straightforward to rearrange to yield Equation 1.

There are two restrictions noted by Mitchell et al. to this design equation. First, the exposed length L should not exceed 1.5 × H, otherwise the net weight will be too high and the cement bonds could be crushed (according to correlations between UCS and bond crushing observed in oedometer tests on sands). This is probably rarely a practical concern as most often exposed backfill faces are taller than they are wide (e.g., for long hole and Alimak stoping methods). The second restriction is that H needs to be no smaller than w tan(45°+$\varphi$/2) where $\varphi$ is the angle of internal friction. This restriction is motivated by the notion that at failure a sliding plane may develop starting at the base of the exposed sidewall and extending up at an angle (45°+$\varphi$/2) to the contact wall opposite the exposed wall. This is a curious restriction for two reasons: first, the assumption of internal failure at the critical angle (45°+$\varphi$/2) is contradictory to the assumption $c_b$ = ½ UCS which inherently implies $\varphi$ = 0; second, the development of Equation 1 as explained above on the basis of net weight does not require any assumption of a kinematically admissible sliding failure plane through the backfill. Furthermore, the essential simplicity of determining UCS without also determining the corresponding c and $\varphi$ is lost if one wishes to strictly adhere to the geometric restriction.

Regardless of these restrictions (which, as noted, are probably moot for many practical backfill design applications), the origins of the $c_b$ = ½ UCS assumption need to be explored. In their 1982 paper the authors present a traditional Mohr's stress space diagram with test results from direct shear and UCS tests, reproduced here as Figure 1 with Mohr's circles at failure superposed for the UCS tests. There are two materials, one with UCS just over 100 kPa and one with UCS just under 200 kPa. The relatively weak UCSs were intentional because weak materials were required to appropriately scale with the model geometry used in the laboratory backfill simulations. For the stronger material (UCS ~200 kPa) the Mohr-Coulomb failure envelope for the direct shear tests at "large strain" appears to be consistent

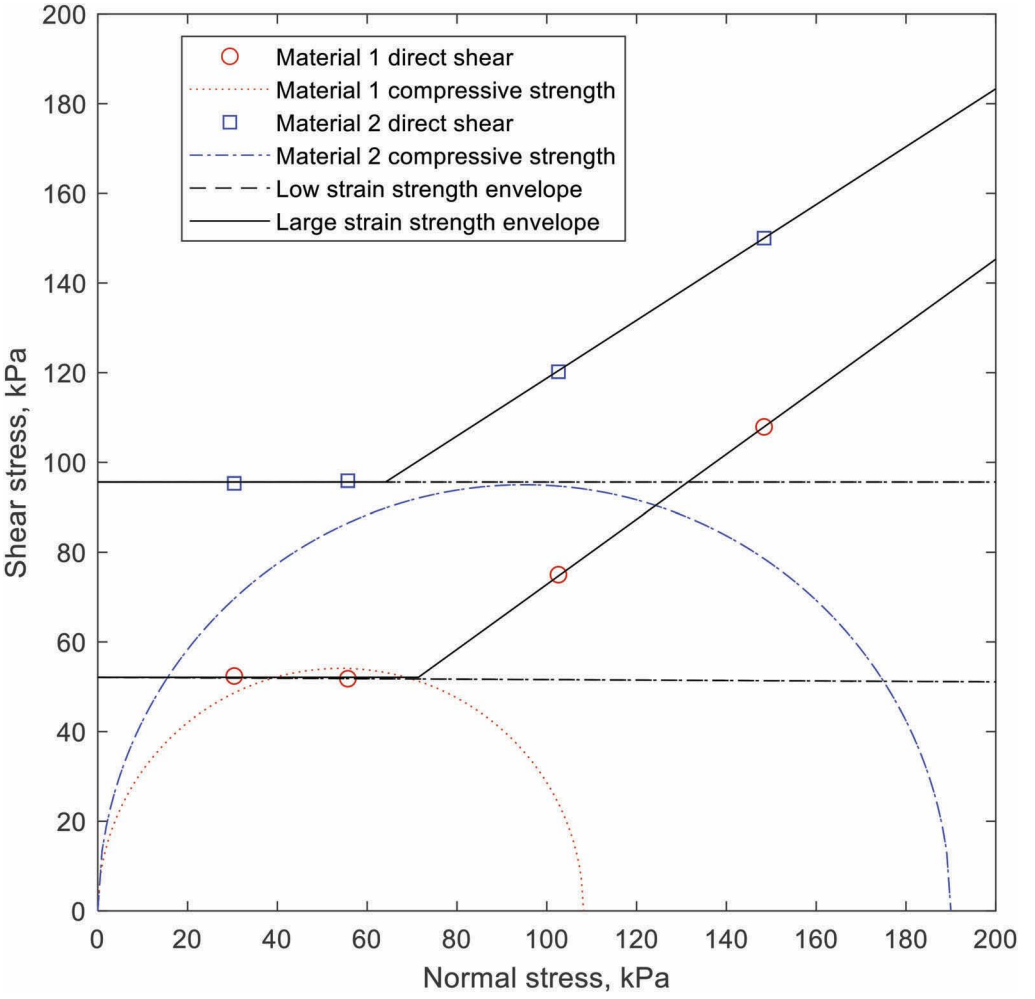


Figure 1. Strength envelopes for materials tested by Mitchell et al. (1982) (adapted from the original).

with (i.e., tangential to) the Mohr's failure circle for the UCS; however, for the weaker material it is clearly not. The direct shear test results at "small strain" and for normal stresses less than about ½ UCS do indeed seem to show a constant shear strength equal to about ½ UCS, but stress-displacement results are never shown to clearly identify what is meant by "small strain" (probably because a very non-standard direct shear test method was used, for which obtaining shear displacements might have been difficult).

The way the researchers obtained relatively weak UCS values was by testing at very early ages, well before 28 days, and so it is not clear how well the hydration products had formed within the modelled backfill materials. Given the uncertainties about the materials, the strength testing methods, and the very unusual failure envelopes, it should be surprising that the resulting design formula (Equation 1) is so widely used without further material testing being undertaken to ascertain the validity of the fundamental assumption, $c_b$ = ½ UCS.

To address this lack of material testing issue, a comprehensive set of quality laboratory tests was undertaken on a particular CPB from Williams mine. Conventional direct shear, specialty UCS for paste backfill, and a novel direct tension test method were used and will be described

in the next section. It is important that these tests be carried out at appropriate normal stress levels. From the previous discussion of how Equation 1 can be rationalized based on net self-weight, the vertical stress through the fill mass will always be less than the UCS obtained from Equation 1. If some reasonable in situ stress ratio is assumed for localized areas within the backfill, then the confining stress should also be less than the UCS. Note that the point of tangency to Mohr's failure circle for the UCS test defines the normal and shear stresses acting on the inclined failure plane through the UCS sample: therefore, a UCS test sample has a non-zero compressive stress on its failure plane, and so does *not* represent failure in a truly "unconfined" condition. This is further addressed in the next section.

## 3 STRENGTH TESTING

This section describes the materials tested, the test methods, and the strength envelopes determined from the tests. Additional details and test results can be found in Pan (2019).

### 3.1 *Materials tested and sample preparation prior to testing*

The CPB materials tested come from Barrick Gold Corp.'s Williams mine, located on the north shore of Lake Superior near the town of Marathon, Ontario. The mineral deposit is finely disseminated gold in low-sulfide Canadian Shield host rock, and the resulting tailings are classified as non-plastic silt. The maximum particle size is less than 1 mm; the $D_{60}$ is 0.030 mm and the $D_{10}$ is 0.003 mm, giving $C_U = 10$; and 45% by weight pass 0.020 mm which is greater than the generally accepted 15% minimum as one of the qualifying paste backfill criteria. CPB is made by preparing the tailings with Ordinary (or Normal, or General Use, or Type 10) Portland Cement and mine process water (the strongest ionic concentrations of which are Na and S at about 9 and 7 mmol/l respectively). Quoted binder contents are based on weight of binder divided by weight of dry tailings. Water content is consistent at 38% on a mass of water divided by mass of solids (tailings + binder) basis (the common definition used in geotechnical engineering), which is equivalent to 27.5% on a mass of water divided by total mass basis (the common definition used in backfill design).

CPB samples are prepared by mixing the constituent materials using a hand blender for 10 minutes, then placed into molds specific to each test method (Figure 2) being careful to avoid air entrainment. The samples are submerged for 1 day to prevent oxidation, then removed from the molds and returned to the water to continue curing until testing time. This effectively eliminates oxidation of the sulfur-bearing minerals, keeps the samples saturated, and eliminates potential suction development due to "self-desiccation" effects during hydration (Simms and Grabinsky, 2009). The tested samples were observed to be homogeneous and had bulk properties consistent with field samples (Grabinsky et al., 2013, 2014).

### 3.2 *Uniaxial compression testing*

The sample mold helps ensure ideal cylindrical geometry. The ends are "polished" on glass to remove irregularities prior to testing. Uniaxial compression testing was conducted with the sample under water, compressed at constant vertical strain of 1% per minute (average 0.65 mm/min). The 1% per minute test rate was determined in many previous research projects on the same material to be sufficiently slow to neutralize internal water pressures/suctions uniformly within the sample when tested under water.

### 3.3 *Direct shear testing*

The sample molds result in cured blocks that fit tightly into the standard direct shear split box for the equipment used, and these were then tested according to ASTM

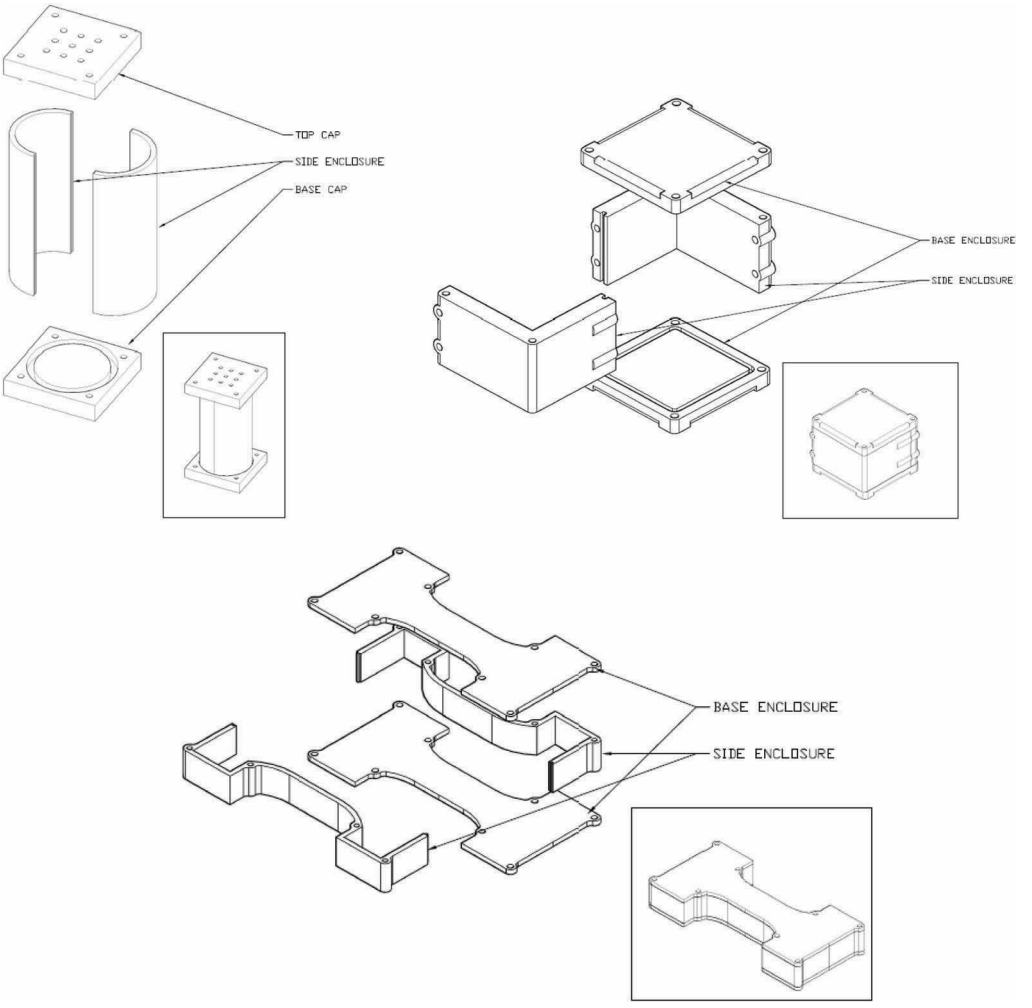


Figure 2. Sample molds for curing specimens for UCS (top left), direct shear (top right), and uniaxial tension (bottom).

Standard D3080: Standard Test Method for Direct Shear Test of Soils Under Consolidated Drained Conditions. The normal stresses ranged from 1 to 210 kPa which covered the desired range compared to the UCS, as discussed previously. The sample enclosure was filled with water during the test, similar to the UCS testing. The horizontal displacement rate was 0.5 mm/min which based on previous tests (Veenstra, 2013) was deemed to be sufficiently slow to neutralize pore pressures/suctions uniformly within the sample when tested under water.

### 3.4 *Uniaxial tension testing*

The uniaxial tension testing employed a novel test device illustrated in Figure 3. The sample mold for the "dog-bone" shaped specimen is shown in Figure 2. The upper portion of the apparatus bears on the lower protrusions of the specimen, and the lower (base) portion bears on the top protrusions. In this way, when the assembly is placed in a loading frame the applied compression is converted into tension within the specimen. The load

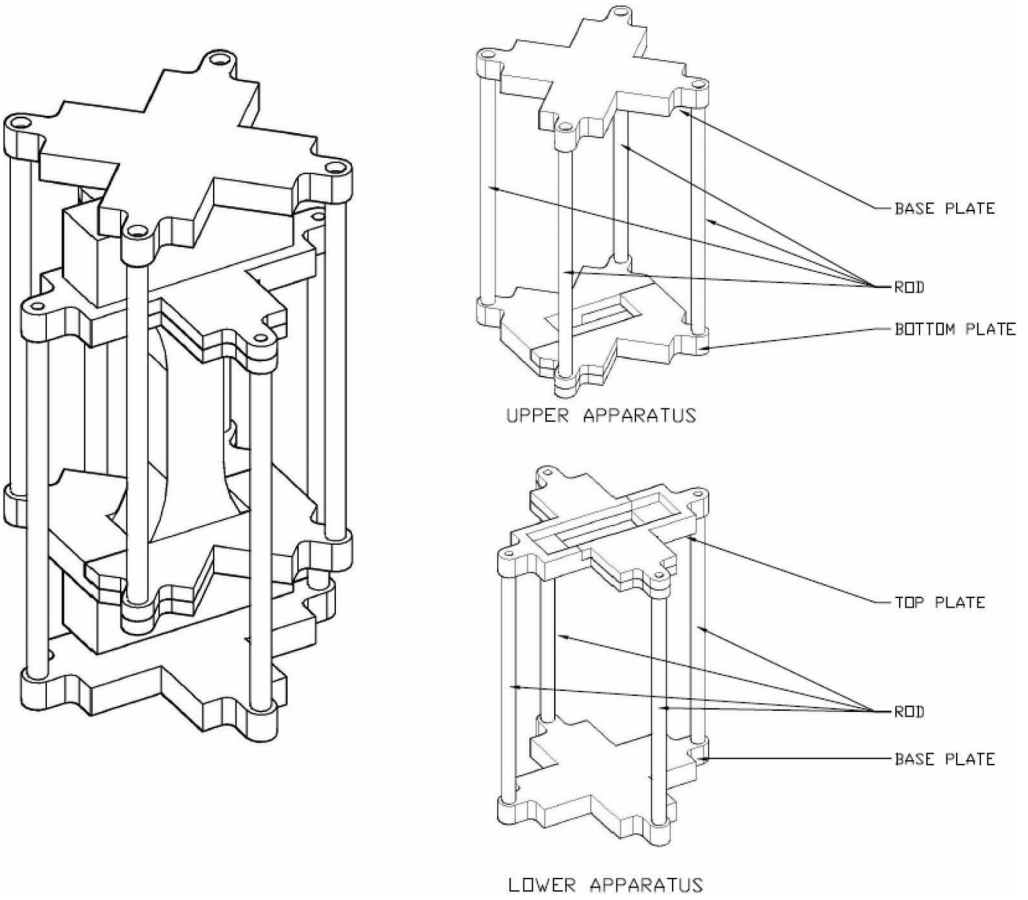


Figure 3. Novel uniaxial tension testing device for dog-bone shaped specimen.

frame is run in displacement control at 0.5 mm/min and the resulting tensile stress development to failure is very stable. The sample breaks horizontally at the specimen's mid-section, such that the failure surface is normal to the tension direction. These tests were not conducted under water, but this is thought to be not as important as for the other test methods due to the comparatively discrete nature of the failure surface and relatively small displacement to failure.

### 3.5 *Test results and strength envelopes*

Figure 4 shows testing results for 28-day cure times at 6.9% and 9.7% binder contents. The direct shear results (dot markers) exhibit good linearity and a Mohr-Coulomb envelope is fit to this data. The Mohr's failure circles for the UCS tests are closely tangent to this envelope, indicating good agreement between the two test methods. The Mohr's failure circles for the uniaxial tension tests are also generally tangent to the envelope, however, the actual failure surfaces are perpendicular to the direction of tension loading and so the corresponding envelope is better represented by a tensile cut-off. Regardless, it appears reasonable to extend the Mohr-Coulomb linear failure surface into the tensile range, as shown. Note that the point of tangency of the UCS circle occurs at a normal stress ~ ¼ UCS, and so the UCS does not represent failure in a truly "unconfined" condition. The direct shear tests, however, provide the

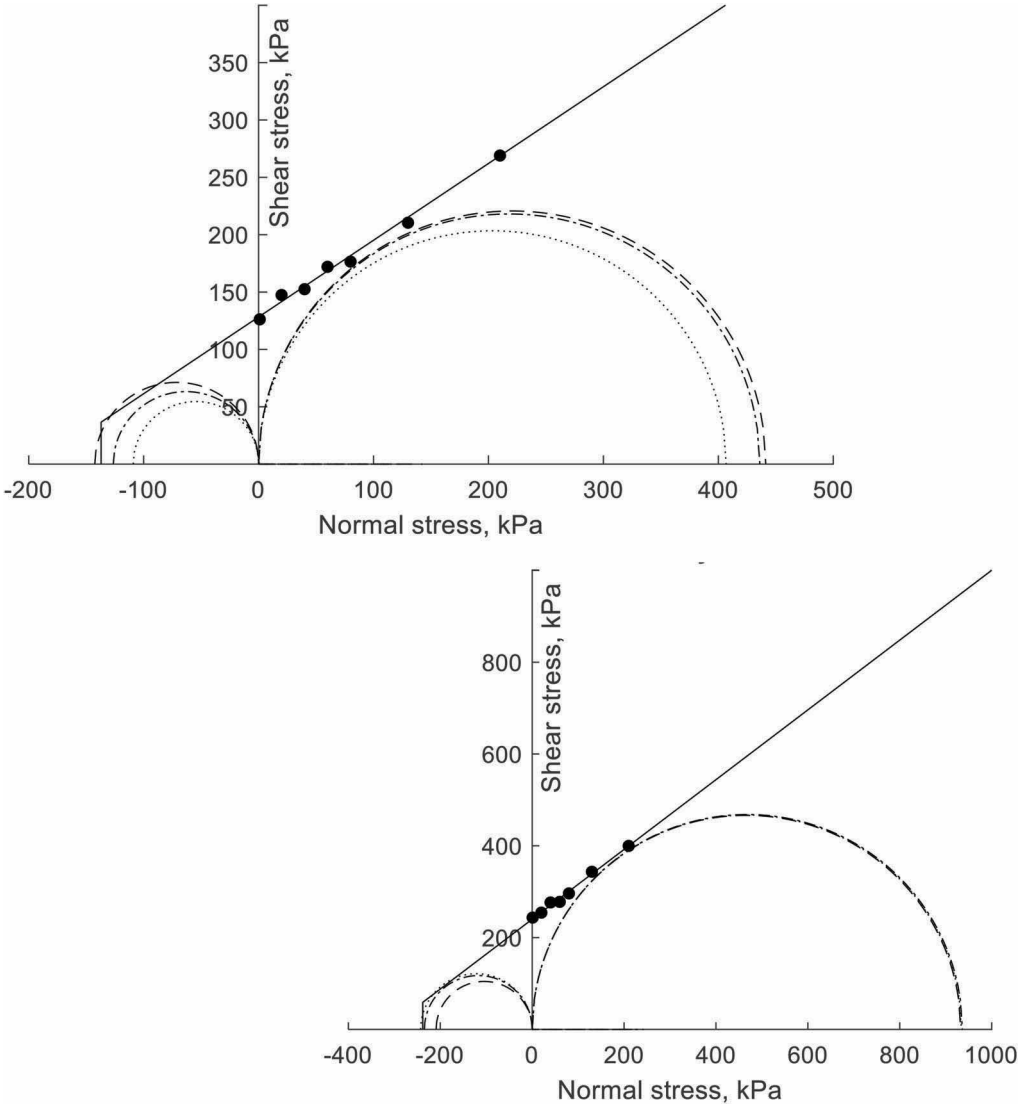


Figure 4. 28-day strength test results for 6.9% (top) and 9.7% (bottom) binder contents. Mohr's failure circles for uniaxial compression (3 tests each) and uniaxial tension (3 tests each); and dot markers for direct shear (7 test each).

additional evidence for actual cohesion (shear stress at zero confining stress) and failure shear stresses at normal stress up to the UCS tangent, and beyond.

## 4 IMPLICATIONS FOR EXPOSED SIDEWALL STRENGTH DETERMINATION

The failure envelopes just presented contrast starkly with the $c_b$ = ½ UCS criterion suggest by Mitchell et al. (1982). Had the materials not been tested under water, and had they been tested quickly, it might be that any dilation tendency would lead to suction and larger apparent shear resistance, but this would not be indicative of actual material behaviour.

Given that $c_b$ = ½ UCS is not an appropriate strength assumption for the Williams CPB material tested in this study (and, very likely not appropriate for similar CPBs made from non-plastic silty tailings) the obvious question arises: what are the implications for exposed backfill sidewalls designed based on Equation 1? This section explores an alternate solution based on the identified Mohr-Coulomb failure criterion and considers generalized design examples.

### 4.1 *Alternative strength determination procedure*

For a Mohr-Coulomb (c-φ) material with no pore water pressure, the shear stresses generated on the sidewalls are no longer constant but instead depend on the normal stress and the strength parameters, and so the vertical stress with depth z below the top backfill surface (again assuming only the two end walls remain in contact) can be written.

$$\sigma_v(z) = \sigma_{vmax}\left(1 - \exp\left(-\frac{z}{\frac{1}{2}L}K\tan\phi\right)\right) \tag{2}$$

where $\sigma_{vmax} = \frac{\gamma\frac{1}{2}L - c}{K\tan\phi}$ is the asymptotic value at large z and K is the horizontal stress ratio. Both $\sigma_{vmax}$ and the decay exponent depend on the term Ktanφ. This term is reasonably insensitive to the assumed value of φ over the range expected for backfills. In the active condition $K_a\tan\varphi \approx 0.2$ and in the at-rest condition $K_o\tan\varphi \approx 0.3$. These are the likely limiting cases for preliminary analyses.

For practical cases the height of backfill is finite and so z = H. From the construction of the Mohr's diagram, UCS can be related to c and φ using UCS = c 2cosφ/(1-sinφ). Following the process outlined in section 1 for the net weight analysis, UCS = $\sigma_v$(z=H) and making the substitutions into Equation (2) and simplifying results in.

$$UCS = \gamma\frac{1}{2}L\left[\frac{\tan\phi}{1 - \exp\left(-\frac{H}{\frac{1}{2}L}K\tan\phi\right)} + \frac{1-\sin\phi}{2\cos\phi}\right]^{-1} \tag{3}$$

For the material test results presented in the previous section ϕ = 37°; and for the active and at-rest states ($K_a$ and $K_o$) the UCS expressions reduce to the following cases:

Active, ϕ = 37°

$$UCS = \frac{1}{2}\gamma L\left[\frac{0.19}{1 - \exp\left(-0.38\frac{H}{L}\right)} + 0.25\right]^{-1} \tag{4}$$

At-rest, ϕ = 37°

$$UCS = \frac{1}{2}\gamma L\left[\frac{0.30}{1 - \exp\left(-0.60\frac{H}{L}\right)} + 0.25\right]^{-1} \tag{5}$$

For very tall stopes, H ≫ L, the above expressions evaluate to UCS = 1.02γL, 0.86γL, 1.14γL, and 0.91γL, respectively, so the range agrees with the Mitchell et al. solution (i.e., the second form presented in Equation 1) to within ±14% for the H ≫ L case. More general cases are considered in the next section.

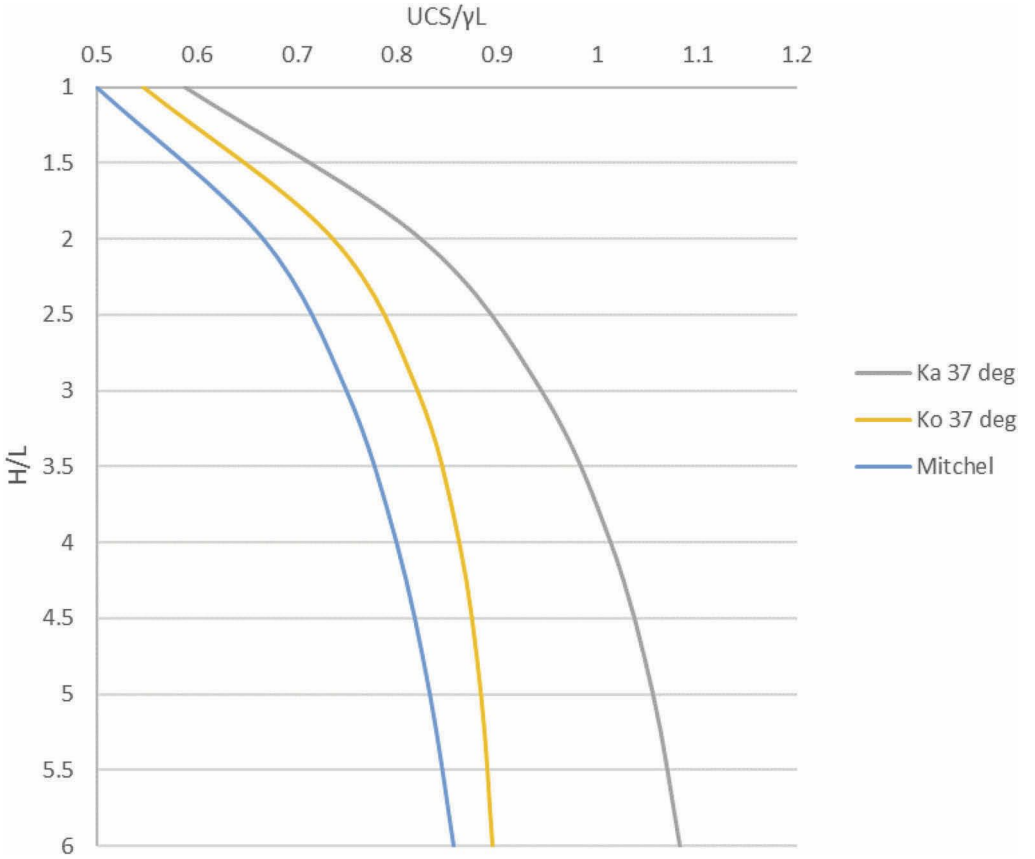


Figure 5. Comparison of Mitchell's predicted normalized strength requirement versus the friction solutions presented in Equations 4 and 5.

### 4.2 *General comparisons*

The second form of Mitchell's solution (Equation 1) can be normalized in terms of UCS/γL and H/L (in fact, this was the normalization used in their paper for comparing analytic predictions with laboratory model data). Figure 5 uses this normalization to compare the predicted normalized strength based on Mitchell's solution (i.e., $c_b$ = ½ UCS), with the predictions based on Equations 4 and 5 for the material tested in this work. In both cases the frictional solutions result in higher predicted UCS, because the assessed shear resistance in the upper portion of the stope has shear resistance less than ½ UCS and so the net weight is greater at the base than would be the case for the constant $c_b$ assumption. The differences are greater for the Ka assumption than for the Ko assumption, because the horizontal stress reaction is less for Ka than for Ko. The largest relative difference occurs for the Ka condition and for H/L between about 3 and 5, where the UCS based on Equation 4 is about 25% higher than the Mitchell et al. solution. The largest relative difference for the Ko condition occurs for H/L between about 1 and 2.5, where the UCS based on Equation 5 is about 10% higher than the Mitchell et al. solution.

## 4 CONCLUSION

The detailed laboratory test results presented in this work provide compelling evidence that the Williams CPB, and by extension probably most other CPBs made from non-plastic silty tailings, follow a Mohr-Coulomb (c-φ) failure envelope. This result contrasts starkly with the constant strength failure envelope ($c_b$ = ½ UCS) assumed in the generally accepted Mitchell et al. (1982) solution for the required UCS of a backfill with exposed sidewall.

Following the Mitchell et al. net weight approach, a generalized solution was developed to find the required UCS based on the c-φ failure envelope. Compared to the Mitchell solution, the required UCS determined using the frictional solutions could be up to 10% to 25% higher. However, this difference likely lies well within the range of Safety Factors used at most mines. Therefore, it should not be surprising that backfill designs based on the Mitchell's solution generally perform adequately well; however, the actual Safety Factors at these mines might be somewhat less generous than assumed. These currently "subtle" differences should nevertheless be kept in mind, as mines continue to strive for greater efficiencies and use less generous Safety Factors.

The quantified strength envelope could also have significance to the design of sill mats in undercut mining, where the flexure mode dominates for relatively thin mats (span/depth > 1; Pakalnis et al., 2005) and the design criterion is based on tensile strength which is notoriously difficult to determine for cemented paste backfills (Johnson et al., 2015).

## ACKNOWLEDGEMENTS

The material testing shown in this paper was carried out by the second author during his MASc Thesis research at the University of Toronto, funded through a Natural Sciences and Engineering Research Council (NSERC) Discovery Grant to the first author.

## BIBLIOGRAPHY

ASTM Standard D3080: Standard Test Method for Direct Shear Test of Soils Under Consolidated Drained Conditions.

Grabinsky, M. W., Bawden, W. F., Simon, D., Thompson, B. T., & Veenstra, R. L. 2013. In situ properties of cemented paste backfill from three mines. *Proceedings of the 2013 Canadian Geotechnical Conference, GeoMontreal 2013*. Montreal. Canadian Geotechnical Society.

Grabinsky, M. W., Simon, D., Thompson, B. D., Bawden, W. F., & Veenstra, R. L. 2014. Interpretation of as-placed cemented paste backfill properties from three mines. *MineFill 2014* (pp. 351–364). Perth: Australian Centre for Geomechanics

Handy, R. L. 1985. The arch in soil arching. *Journal of Geotechnical Engineering*, 111(3), 302–318.

Johnson, J. C., Seymour, J. B., Martin, L. A., Stepan, M., Arkoosh, A., & Emery, T. (2015, November). Strength and elastic properties of paste backfill at the Lucky Friday Mine, Mullan, Idaho. In 49th US Rock Mechanics/Geomechanics Symposium. American Rock Mechanics Association.

Mitchell, R. J., Olsen, R. S., & Smith, J. D. 1982. Model studies on cemented tailings used in mine backfill. *Canadian Geotechnical Journal*, 19(1), 14–28

Pakalnis, R., Caceres, C., Clapp, K., Morin, M., Brady, T., Williams, T., Blake, W. & MacLaughlin, M. (2005). Design spans – underhand cut and fill mining. 107th Annual General Meeting, Canadian Institute of Mining

Pan, A. 2019. *Mechanical properties of Cemented Paste Backfill under low confining stress*. MASc Thesis, University of Toronto. Institutional electronic repository: https://tspace.library.utoronto.ca/

Simms, P., & Grabinsky, M. 2009. Direct measurement of matric suction in triaxial tests on early-age cemented paste backfill. *Canadian Geotechnical Journal*, 46(1), 93–101.

Terzaghi, K. 1967. *Soil Mechanics in Engineering Practice*, John Wiley & Sons. Inc., New York.

Veenstra, R.L., 2013. *A design procedure for determining the in situ stresses of early age cemented paste backfill*. PhD Thesis, University of Toronto. Institutional electronic repository: https://tspace.library.utoronto.ca/handle/1807/36027